Gold nanoring trimers: a versatile structure for infrared sensing

Siew Lang Teo,[1] Vivian Kaixin Lin,[1] Renaud Marty,[2] Nicolas Large,[2,3] Esther Alarcon Llado,[1] Arnaud Arbouet,[2] Christian Girard,[2] Javier Aizpurua,[3] Sudhiranjan Tripathy[1*] and Adnen Mlayah[2]

[1]*Institute of Materials Research and Engineering, A*STAR (Agency for Science, Technology, and Research), 3 Research Link, 117602 Singapore*
[2]*Centre d'Elaboration de Matériaux et d'Etudes Structurales (CEMES/CNRS) and Université de Toulouse, 29 rue Jeanne Marvig, 31055 Toulouse Cedex 4, France*
[3]*Centro de Física de Materiales CSIC-UPV/EHU and and Donostia International Physics Center, Paseo Manuel de Lardizabal 4, Donostia-San Sebastián 20018, Spain*
**tripathy-sudhiranjan@imre.a-star.edu.sg*

Abstract: In this work we report on the observation of surface plasmon properties of periodic arrays of gold nanoring trimers fabricated by electron beam lithography. It is shown that the localized surface plasmon resonances of such gold ring trimers occur in the infrared spectral region and are strongly influenced by the nanoring geometry and their relative positions. Based on numerical simulations of the optical extinction spectra and of the electric near-field intensity maps, the resonances are assigned to surface plasmon states arising from the strong intra-trimer electromagnetic interaction. We show that the nanoring trimer configuration allows for generating infrared surface plasmon resonances associated with strongly localized electromagnetic energy, thus providing plasmonic nanoresonators well-suited for sensing and surface enhanced near-infrared Raman spectroscopy.

OCIS codes: (220.0220) Optical design and fabrication; (220.4241) Nanostructure Fabrication; (160.4760) Optical Properties; (240.6680) Surface Plasmons.

References and links

1. S. A. Maier, M. L. Brongersma, P. G. Kik, S. Meltzer, A. A. G. Requicha, and H. A. Atwater, "Plasmonics - a route to nanoscale optical devices," Adv. Mater. **13**(19), 1501–1505 (2001).
2. A. V. Kabashin, P. Evans, S. Pastkovsky, W. Hendren, G. A. Wurtz, R. Atkinson, R. Pollard, V. A. Podolskiy, and A. V. Zayats, "Plasmonic nanorod metamaterials for biosensing," Nat. Mater. **8**(11), 867–871 (2009).
3. Y. B. Zheng, Y. W. Yang, L. Jensen, L. Fang, B. K. Juluri, A. H. Flood, P. S. Weiss, J. F. Stoddart, and T. J. Huang, "Active molecular plasmonics: controlling plasmon resonances with molecular switches," Nano Lett. **9**(2), 819–825 (2009).
4. K. Kneipp, Y. Wang, H. Kneipp, L. T. Perelman, I. Itzkan, R. R. Dasari, and M. S. Feld, "Single molecule detection using surface-enhanced Raman scattering," Phys. Rev. Lett. **78**(9), 1667–1670 (1997).
5. S. Lal, N. K. Grady, J. Kundu, C. S. Levin, J. B. Lassiter, and N. J. Halas, "Tailoring plasmonic substrates for surface enhanced spectroscopies," Chem. Soc. Rev. **37**(5), 898–911 (2008).
6. J. Aizpurua, P. Hanarp, D. S. Sutherland, M. Käll, G. W. Bryant, and F. J. García de Abajo, "Optical properties of gold nanorings," Phys. Rev. Lett. **90**(5), 057401 (2003).
7. E. M. Larsson, J. Alegret, M. Käll, and D. S. Sutherland, "Sensing characteristics of NIR localized surface plasmon resonances in gold nanorings for application as ultrasensitive biosensors," Nano Lett. **7**(5), 1256–1263 (2007).
8. M. G. Banaee, and K. B. Crozier, "Gold nanorings as substrates for surface-enhanced Raman scattering," Opt. Lett. **35**(5), 760–762 (2010).
9. A. M. Funston, C. Novo, T. J. Davis, and P. Mulvaney, "Plasmon coupling of gold nanorods at short distances and in different geometries," Nano Lett. **9**(4), 1651–1658 (2009).
10. W. Rechberger, A. Hohenau, A. Leitner, J. R. Krenn, B. Lamprecht, and F. R. Aussenegg, "Optical properties of two interacting gold nanoparticles," Opt. Commun. **220**(1-3), 137–141 (2003).
11. P. K. Jain, and M. A. El-Sayed, "Noble metal nanoparticle pairs: effect of medium for enhanced nanosensing," Nano Lett. **8**(12), 4347–4352 (2008).
12. B. Willingham, D. Brandl, and P. Nordlander, "Plasmon hybridization in nanorod dimmers," Appl. Phys. B **93**(1), 209–216 (2008).

#132979 - $15.00 USD Received 5 Aug 2010; revised 26 Sep 2010; accepted 28 Sep 2010; published 6 Oct 2010

13. P. Nordlander, C. Oubre, E. Prodan, K. Li, and M. I. Stockman, "Plasmon hybridization in nanoparticle dimmers," Nano Lett. **4**(5), 899–903 (2004).
14. C. E. Talley, J. B. Jackson, C. Oubre, N. K. Grady, C. W. Hollars, S. M. Lane, T. R. Huser, P. Nordlander, and N. J. Halas, "Surface-enhanced Raman scattering from individual au nanoparticles and nanoparticle dimer substrates," Nano Lett. **5**(8), 1569–1574 (2005).
15. A. Kinkhabwala, Z. F. Yu, S. H. Fan, Y. Avlasevich, K. Mullen, and W. E. Moerner, "Large single-molecule fluorescence enhancements produced by a bowtie nanoantenna," Nat. Photonics **3**(11), 654–657 (2009).
16. Z. Zhang, A. Weber-Bargioni, S. W. Wu, S. Dhuey, S. Cabrini, and P. J. Schuck, "Manipulating nanoscale light fields with the asymmetric bowtie nano-colorsorter," Nano Lett. **9**(12), 4505–4509 (2009).
17. J. A. Fan, C. H. Wu, K. Bao, J. Bao, R. Bardhan, N. J. Halas, V. N. Manoharan, P. Nordlander, G. Shvets, and F. Capasso, "Self-assembled plasmonic nanoparticle clusters," Science **328**(5982), 1135–1138 (2010).
18. M. Hentschel, M. Saliba, R. Vogelgesang, H. Giessen, A. P. Alivisatos, and N. Liu, "Transition from isolated to collective modes in plasmonic oligomers," Nano Lett. **10**(7), 2721–2726 (2010).
19. J. B. Lassiter, H. Sobhani, J. A. Fan, J. Kundu, F. Capasso, P. Nordlander, and N. J. Halas, "Fano resonances in plasmonic nanoclusters: geometrical and chemical tunability," Nano Lett. **10**(8), 3184–3189 (2010).
20. V. K. Lin, S. L. Teo, R. Marty, A. Arbouet, Ch. Girard, E. Alarcon-Llado, S. H. Liu, M. Y. Han, S. Tripathy, and A. Mlayah, "Dual wavelength sensing based on interacting gold nanodisk trimers," Nanotechnology **21**(30), 305501 (2010).
21. F. J. García de Abajo, and A. Howie, "Retarded field calculation of electron energy loss in inhomogeneous dielectrics", Phys. Rev. Lett. **80**, 5180–5183 (1998); "Retarded field calculation of electron energy loss in inhomogeneous dielectrics," Phys. Rev. B **65**, 115418 (2002).
22. P. B. Johnson, and R. W. Christy, "Optical constants of the nobel metals," Phys. Rev. B **6**(12), 4370–4379 (1972).
23. K. L. Wustholz, A. I. Henry, J. M. McMahon, R. G. Freeman, N. Valley, M. E. Piotti, M. J. Natan, G. C. Schatz, and R. P. Van Duyne, "Structure-activity relationships in gold nanoparticle dimers and trimers for surface-enhanced Raman spectroscopy," J. Am. Chem. Soc. **132**(31), 10903–10910 (2010).
24. B. Auguié, and W. L. Barnes, "Diffractive coupling in gold nanoparticle arrays and the effect of disorder," Opt. Lett. **34**(4), 401–403 (2009).
25. C. Girard, "Near fields in nanostructures," Rep. Prog. Phys. **68**(8), 1883–1933 (2005).
26. I. Romero, J. Aizpurua, G. W. Bryant, and F. J. García De Abajo, "Plasmons in nearly touching metallic nanoparticles: singular response in the limit of touching dimers," Opt. Express **14**(21), 9988–9999 (2006).
27. J. Aizpurua, G. W. Bryant, L. J. Richter, F. J. García de Abajo, B. K. Kelley, and T. Mallouk, "Optical properties of coupled metallic nanorods for field-enhanced spectroscopy," Phys. Rev. B **71**(23), 235420 (2005).
28. J. B. Lassiter, J. Aizpurua, L. I. Hernandez, D. W. Brandl, I. Romero, S. Lal, J. H. Hafner, P. Nordlander, and N. J. Halas, "Close encounters between two nanoshells," Nano Lett. **8**(4), 1212–1218 (2008).

1. Introduction

The patterning of metallic nanostructures has recently attracted considerable attention in the areas of photonics, electronics, and biosensing [1–5]. Majority of research work is focused on the fabrication of well-controllable and highly-ordered noble metal nanostructures using advanced top-down lithography techniques. Among various noble metal nanostructures, gold nanorings have shown promising applications in the area of plasmon-induced sensing [6–8]. The optical properties of gold nanorings fabricated by colloidal lithography exhibit tunable localized surface plasmon resonance (LSPR) in the visible to near-infrared spectral region [6]. The tunability is obtained by changing the ratio of the ring wall thickness to ring outer diameter. This study was complemented by LSPR sensing and recently by surface-enhanced Raman scattering (SERS) [7, 8].

The closely-spaced nanoshell or nanoparticle arrays are also shown as suitable templates for SERS as well as for surface-enhanced infrared absorption (SEIRA) spectroscopy, where large electromagnetic field enhancements at selective spatial locations can be tuned by controlling the small interparticle distances. In such interacting noble metal nano-objects, the surface plasmon resonances of individual object hybridize and form red-shifted bands in the near-infrared and mid-infrared spectral regions originating from combinations of quadrupolar and dipolar resonances [9–16]. Exploiting the interaction between metal nanoparticles in complex geometries, like hexamers and heptamers, has led to the concept of plasmonic oligomers with tailored optical properties [17–19].

Nanosdisk-based plasmonic oligomers were recently investigated in several works [17–20]. In a previous work, we investigated the surface plasmon properties of nanodisk trimers [20] and pointed out the effects of interactions between nanodisks within a trimer and between trimers. So far, only few studies address plasmonic oligomers with nanorings as elementary bricks. Because the electromagnetic field is localized around the ring wall, in the

#132979 - $15.00 USD Received 5 Aug 2010; revised 26 Sep 2010; accepted 28 Sep 2010; published 6 Oct 2010

case of closely spaced ring oligomers, the hybridization of the surface plasmon resonances is expected to be more pronounced than in equivalent nanodisk based oligomers. In addition, the surface plasmon resonances of nanorings are shifted to the infrared with respect to that of equivalent nanodisks. So, in terms of sensing properties, ring-based oligomers should offer a higher sensitivity together with a greater tunability (ring size and wall thickness in addition to ring separation). Moreover, electromagnetic field enhancement in the near-infrared region achieved with interacting nanorings would also be suitable for surface-enhanced near-infrared absorption. The enhancement of optical scattering signal in such trimers could play an increasingly important role in the field of biological sensing due to complementary vibrational analysis of biomolecules combined with LSPR. The fabrication of nanoring-based oligomers is however very challenging since it requires the control of not only the ring size, shape and location but also of the ring wall which should be as thin as the gap between interacting nanorings for optimum surface plasmon hybridization. Reliable fabrication protocol to control local field enhancement in such complex patterns, absolute quantification and understanding of SERS and LSPR mechanisms are not yet well-explored in the case of trimers comprising gold nanorings.

In this study, we focus on the surface plasmon properties of nanoring based trimers. We have fabricated gold nanoring trimers using electron beam lithography (EBL) technique and studied their surface plasmon properties. In particular, we have obtained nanoring trimers with less than 20 nm ring gap spacing, and outer diameter of rings in the range of 120 – 130 nm. The transmission measurements show surface plasmon resonances around 1000, 1560, and 3300 nm. Numerical simulations of the extinction spectra and associated near-field intensity maps are used for the interpretation of the optical experiments. We found that unlike in nanodisk trimers where the two observed surface plasmons resonances are due to intra-trimer and inter-trimer interactions [20], both 1000 and 1560 nm resonances arise from intra-trimer interaction. Whereas the 3300 nm resonance is connected with the inter-trimer interaction. Moreover, we report on sensing experiments showing that the nanoring trimers sensitivity to the optical index of the surrounding medium is nearly three times larger than that of nanodisk trimers with comparable size [20].

2. Experimental

The nanoring trimers are prepared using EBL and thermal evaporation of a gold layer onto quartz substrates. The square lattice array of rings and ring trimers are prepared over a 100 μm × 100 μm area. To obtain different nanoring geometry (for example, outer diameter of 120 and 130 nm with a fixed ring wall thickness), we have first designed the pattern masks using e-beam resist. In our case, the e-beam resist is ZEP5A (1:3), where ZEP consists of a copolymer of -chloromethacrylate and –methylstyrene. The resist is spun onto the quartz substrates followed by a soft baking at 180 °C for 2 mins. The EBL is performed using an Elinoix ELS 7000 set up at 100 kV. In order to prepare nanorings or ring trimers, we have used 60 pA beam current with a dose of 360 $\mu C/cm^2$. The resist development is done in oxylene for 30 seconds. The patterned templates are then loaded into the evaporation chamber for deposition of a very thin layer of chromium (that improves the structural stability of the pattern) followed by a desired thickness of gold (Cr/Au: 3/25 nm). The lift-off process to realize gold nanopatterns is achieved using dimethyl sulfoxide. Series of scanning electron microscopy (SEM) experiments are performed to obtain optimized thickness and geometry of square-lattice patterned gold nanoring, nanoring dimers, and trimers. The processing conditions are tuned to achieve nearly touching rings or closely-spaced rings within the trimer geometry.

The optical properties of these 2D arrays of gold nanoring trimers are studied by microscopic transmission and reflection measurements. The incident light is unpolarized and the spectra are collected using a CRAIC micro-spectrophotometer where light transmitted by the nanoring trimers is dispersed to the spectrometer through a 36X long distance microscope objective with 0.5 numerical aperture. The probed area is around 250 μm^2 spot and the number of probed nano-objects is about 1600 in the case of ring trimers with a 400 nm pitch.

#132979 - $15.00 USD Received 5 Aug 2010; revised 26 Sep 2010; accepted 28 Sep 2010; published 6 Oct 2010

The transmission data are normalized with respect to spectra acquired only from the quartz substrate. The LSPR wavelengths showed no dependence on the probed point of the 100 µm × 100 µm area except at the boundaries of this area. All sensing measurements were performed at the center of this area where the trimers showed a good uniformity. For LSPR sensing experiments, we have carried out transmission measurements on our gold ring trimers by varying the refractive index of the surrounding medium.

3. Results and discussion

Before forming ring trimers, we have optimized the fabrication of individual nanorings as well as ring dimers with different periodicity in a square lattice format. Figures 1a and 1b show SEM images of individual gold nanorings with different outer diameters (120 ± 5 nm and 130 ± 5 nm) but with a similar ring wall thickness of about 33 nm. The ring height is about 24 ± 2 nm, which is confirmed by the atomic force microscopy measurements (Fig. 1c and 1d); the separation pitch between individual rings is about 240 nm.

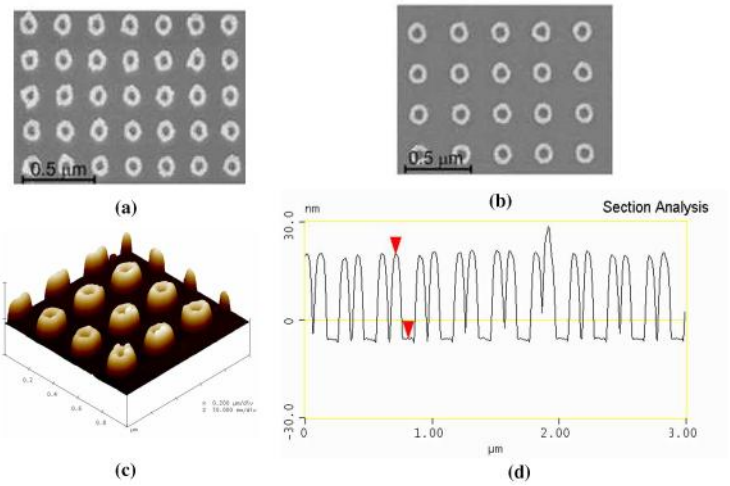

Fig. 1. SEM image of gold nanorings NR120 and NR130, prepared by e-beam lithography and with outer diameter of 120 ± 3 nm (a) and 130 ± 3 nm (b), respectively. Both sets of rings have similar wall thickness of about 33 ± 3 nm. (c) The typical 3D AFM micrograph of the rings NR130 showing rounded shape of top ring wall. (d) An AFM section profile of the gold nanorings array showing the top rounded shape ring wall.

The corresponding optical density spectra of nanorings, deduced as log (1/T) (T being the transmission), are shown in Fig. 2. The spectra reveal a strong optical resonance in the near-infrared spectral region, whose wavelength red-shifts with increasing ring dimensions. In order to determine the influence of the ring characteristics we have calculated the extinction cross section of gold nanorings using the Boundary Element Method (BEM) in a full electromagnetic calculation [6, 21], including retardation effects. The wavelength dependence of the dielectric properties of gold was taken from Johnson and Christy [22]. The ring diameters and wall thicknesses are those determined from the SEM images (Figs. 1a and 1b). Outer and inner diameters are D_{out}= 130 ± 5 nm, D_{in}= 70 ± 5 nm for NR130 and D_{out}= 120 ± 5 nm, D_{in}= 60 ± 5 nm for NR120. The nanoring is positioned on a quartz substrate and its height is 24 nm including the 3 nm chromium layer at the ring/substrate interface. We found that this Cr layer is responsible for about 15% of the homogeneous width of the LSPR. Figure 2 shows the optical spectra calculated using the BEM in the transmission configuration, i.e. with the incident electric field polarization parallel to the ring plane. The surface plasmon resonance in the simulated spectra (Figs. 2a and 2b) is due to the coupling between the inner and outer walls of the nanoring. This peak corresponds to a symmetric distribution of the surface polarization charges on the ring walls [6]. Its wavelength strongly depends on the ring size.

#132979 - $15.00 USD Received 5 Aug 2010; revised 26 Sep 2010; accepted 28 Sep 2010; published 6 Oct 2010

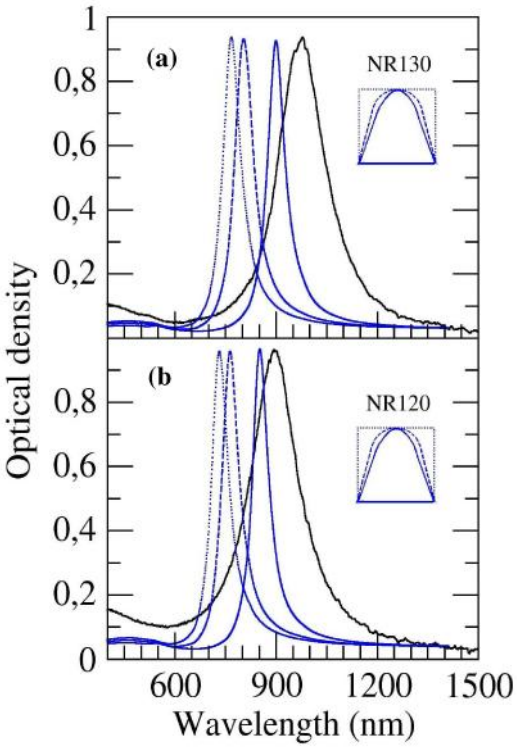

Fig. 2. Measured (black) and calculated (blue) optical density spectra of nanorings NR130 (D_{out}= 130 nm, D_{in}= 70 nm) and NR120 (D_{out}= 120 nm, D_{in}= 60 nm). Spectra were simulated and measured in the transmission configuration. The optical density is obtained as log (1/T); where T is the transmission. In the inset is depicted a cross section of the ring wall. Flat (dotted lines) and two types of rounded ring wall profiles (dashed and solid lines) are considered in order to show the red-shift of the SPR wavelength when stressing the rounded shape of the ring wall.

Experimentally, we observe a strong extinction peak in the near-infrared spectral region (black line in Fig. 2) whose wavelength is comparable to the one of the simulated symmetric LSPR (blue lines in Fig. 2). In addition, we observe that, as the wall thickness to ring diameter ratio decreases (from sample NR120 to NR130), the resonance red-shifts in agreement with the simulations. This is due to a stronger interaction between the inner and outer walls of the ring [6]. Nevertheless, one can notice that the wavelengths of the simulated extinction peaks are underestimated with respect to the measured ones: 165 nm and 207 nm differences for NR120 and NR130, respectively. It is interesting to understand the origin of this discrepancy, which is around 18.5% for NR120 and 21.2% for NR130 in terms of percentages of the measured resonance wavelengths. Slight distortion of the nanoring to ellipsoidal shape could not completely explain that difference. Indeed, the simulations showed that a small ellipsoidal distortion only increases the resonance linewidth due to degeneracy removal of the folded anti-symmetric surface plasmon modes. In addition, SEM showed no evidence for ellipsoidal distortion of the e-beam lithographied nanorings (Fig. 1a and 1b). However, from the AFM imaging (Fig. 1c) and profiles (Fig. 1d), one can notice that the rings are not ideally flat on top, as those assumed in the previous simulations, but rather exhibit a rounded shape. Therefore, we have simulated the extinction spectra of nanorings assuming a rounded shape resembling the one revealed by AFM (Fig. 1c).

Figure 2 shows the results for nanorings NR120 and NR130 with the same diameters and size of the ring wall but also considering a rounded shape on top (dashed and full lines in Fig. 2). We found that this shape effect is responsible for a red shift of the surface plasmon resonance by about 121 nm and 133 nm, with respect to the case of ideal nanorings with

#132979 - $15.00 USD Received 5 Aug 2010; revised 26 Sep 2010; accepted 28 Sep 2010; published 6 Oct 2010

squared shape on top (dotted lines in Fig. 2), for NR120 and NR130 respectively. Taking into account this shape effect reduces the discrepancy with the experimental resonance wavelengths to 5% and 8% for NR120 and NR130, respectively, stressing the importance of fine geometrical features in the final resonance position. Furthermore, as one can notice from the AFM and SEM images (Fig. 1), the surface of the nanorings exhibits some roughness and defects, which may also affect the LSPR. In addition, a fluctuation of ±3 nm of the ring wall is responsible for ±10.5 nm shift of the surface plasmon wavelength that might explain the small difference between the simulated and measured extinction peak wavelength and linewidth (i.e., inhomogeneous broadening).

In the previous section, we have demonstrated that not only the ring diameter and ring wall thickness, but also the ring shape significantly affects the surface plasmon resonance wavelength. This is important for the understanding of the optical properties of more complex ring-based systems. We now aim to exploit the surface plasmon hybridization in interacting nanorings for a controlled engineering of the optical properties at the nanoscale. To do so, it is necessary to optimize and have a precise control over the positions between nano-objects. In order to create ring trimers with a specific gap between individual rings, we have first optimized the positions of the top two rings in terms of closely-spaced dimers. With an optimized fabrication condition, we could control the spacing between rings as small as 10 nm. Figure 3a (top) shows the SEM imaging of ring dimers with variable gaps. The fabrication protocol of such dimers allowed us to form ring trimers of variable geometry (see bottom SEM images in Fig. 3). With our optimized process conditions, we were able to fabricate ring trimers with 400 nm (Figs. 3c, 3d) and 1000 nm (Fig. 3b) spacing between the centers of the trimers in a square lattice pattern with a good uniformity over the 100 μm x 100 μm area. The outer diameter of the top two rings is 10 nm smaller than that of the bottom ring. This allowed us to form heterotrimers, where the average spacing between the top two rings within a trimer is around 15 nm, for the case of trimers with a 400 nm pitch. For trimers with larger periodicity (1000 nm pitch, Fig. 3b), we can form uniform patterns with nanorings of nearly same outer diameter and gaps. In that case, the average spacing between the top two rings within a trimer was measured to be less than 18 nm.

#132979 - $15.00 USD Received 5 Aug 2010; revised 26 Sep 2010; accepted 28 Sep 2010; published 6 Oct 2010

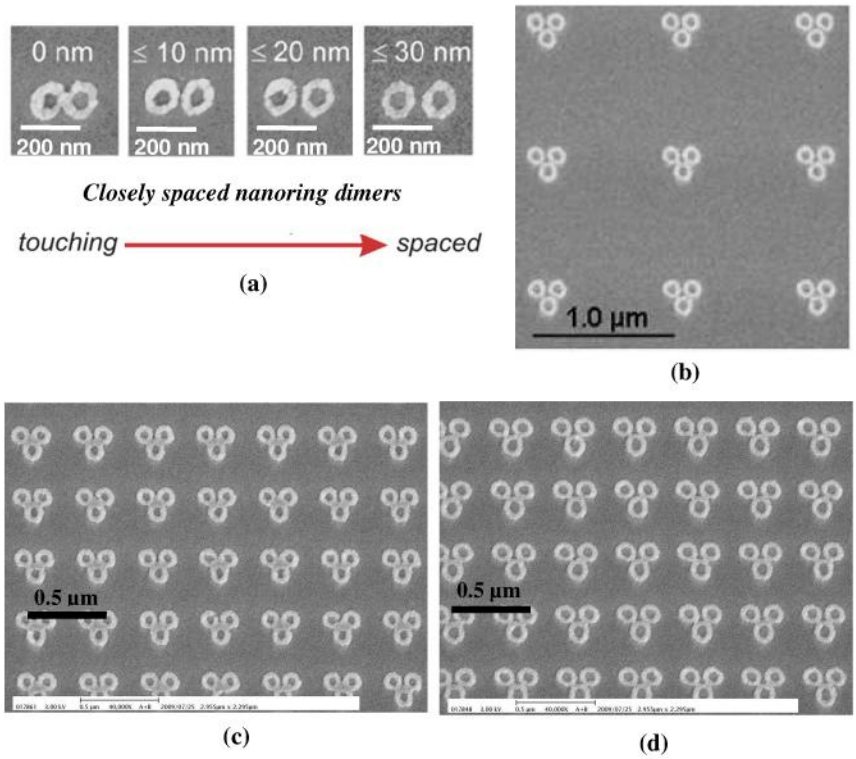

Fig. 3. (a) SEM images of ring dimers with variable gaps (0 to 30 nm) fabricated by EBL and lift-off process. (b) SEM image of nanoring trimers with a large periodicity (1000 nm pitch, isolated trimer with ring diameter 120 nm) and with nearly uniform spacing between top two rings in the trimer geometry. (c) SEM image of nanoring trimer array where the bottom ring outer diameter was kept at 120 nm with ≤15 nm average spacing between top two rings in touching and overlapping situations of ring walls. (d) SEM image of nanoring trimer array with ≤18 nm spacing between top two rings where the bottom ring outer diameter was kept at 130 nm. In the above cases, the ring trimers are arranged in a square lattice pattern with a pitch of 400 nm.

Figure 4 shows typical transmission spectra of the gold ring trimers with 400 nm pitch. We have produced two types of trimer configurations, depending on whether the bottom ring outer diameter is larger or smaller than that of the top two rings (SEM shown in inset of Fig. 4). First, instead of the single resonance found at around 900 nm (Fig. 2) in isolated nanorings, two extinction bands are detected for the trimers (Fig. 4). The bands are separated by several hundreds of nanometers (523 nm and 610 nm for the two cases considered in Fig. 4). This point out the importance of exploiting the interaction between nano-objects in order to generate additional spectral features that may be useful for applications. Second, we show that the engineering of the optical properties of these complex nanoring-based trimers can be performed owing to a precise control of the interaction configuration. Indeed, for the case of heterotrimers with bottom ring outer diameter of about 120 ± 5 nm and top two rings of a comparatively smaller diameter 110 ± 5 nm, we could see extinction bands at 942 nm and 1465 nm while in the reverse case, where we have a smaller bottom ring outer diameter of 110 ± 5 nm and top two rings of higher diameter 120 ± 5 nm, the bands are shifted to 1040 nm and 1650 nm. Due to limitation of our micro-spectrophotometer, we could only record spectral signal up to 1700 nm. However, the spectra clearly depict the wavelength dependence of the observed extinction bands on the relative diameters of the two top and bottom rings.

#132979 - $15.00 USD Received 5 Aug 2010; revised 26 Sep 2010; accepted 28 Sep 2010; published 6 Oct 2010

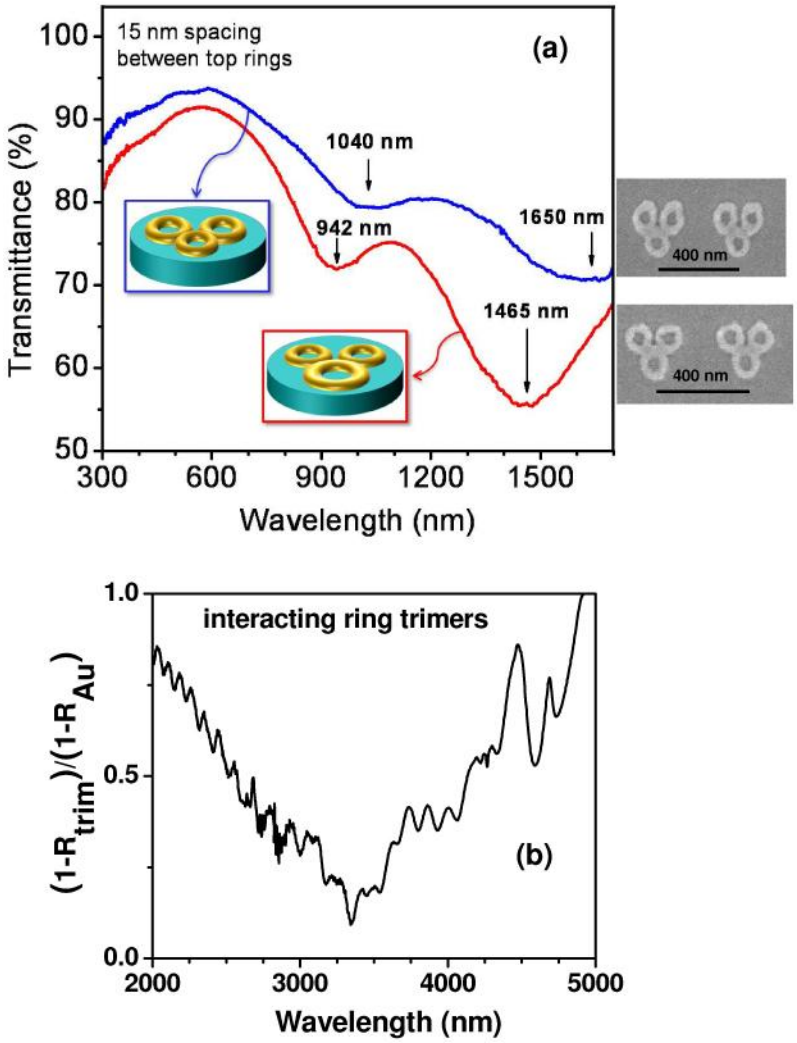

Fig. 4. (a) Experimental tuning of the LSPR peaks by changing the bottom ring outer diameter in the nanoring trimers. The insets are schematic representations of the trimer geometry as well as a representative SEM image for each interacting trimer sample where the average spacing between top rings is around 15 nm. The separation between the trimers is about 400 nm. (b) The transmission (1–R) spectrum of nanoring trimers normalized to that of the spectrum of a 30 nm thick gold layer on quartz. The spectra obtained with a micro-FTIR set up reveals a clear dip around 3300 nm, which we tentatively attribute to the resonance related to the interaction between neighboring trimers.

It must be kept in mind that, in our fabrication protocol, a very thin Cr layer (3 nm) on top of the quartz substrate was used to improve the structural stability of the nanoring trimers. However, this interfacial layer weakens the transmission and somehow compromises the sharpness of the trimer LSPR as deduced from the simulations. Moreover, one can compare the linewidth of the LSPRs in Fig. 2 (rings) and in Fig. 4 (trimers) and can notice the increase of broadening due to interaction between the rings within the trimers. This observation is similar to that recently reported by Wustholz et *al*. [23] for dimers and trimers of Au/SiO_2 core-shell spherical nanoparticles.

Since ring trimers are relatively close in our samples (400 nm pitch), electromagnetic interaction between neighboring trimers should be present and could lead to observations of additional resonances at higher wavelengths. To check the possible presence of such

#132979 - $15.00 USD Received 5 Aug 2010; revised 26 Sep 2010; accepted 28 Sep 2010; published 6 Oct 2010

resonance we have performed micro-FTIR reflectance measurements of the nanoring trimers. The transmission (1–R) spectrum of nanoring trimers is plotted in Fig. 4. We have normalized the spectrum to that of a 30 nm thick gold layer on quartz. The spectrum reveals a clear dip around 3300 nm, which we tentatively attribute to the resonance related to the interaction between neighboring trimers [20]. As a matter of fact, no similar spectral feature was observed in the case of isolated ring trimers (shown in Fig. 3b) certainly because of the large separation between trimers (1 μm).

It is worthwhile to mention that we observed no sharp Bragg diffraction peak in the transmission spectra of our samples, as the one reported by Auguié and Barnes [24]. Such a spectral feature is the signature of long-range diffractive coupling between nano-objects. The reason for the absence of such effect in the spectra of Figs. 2 and 4 lies in the rather small period (400 nm) of our nanostructures as compared to the LSPR wavelengths. In the case of Auguié and Barnes [24], the periodicity was slightly higher and the particles were immersed in a matching index fluid thus allowing for Bragg diffraction to occur.

To get more insight in the nature of the surface plasmons in ring trimers, we have calculated the extinction spectra and the electric near-field intensity maps associated to the main optical resonances of this complex nano-pattern. To achieve this analysis we have used the Green dyadic method because of the low-symmetry of the ring trimer. This method has been used for the modeling of the surface plasmon properties of a variety of metal nanostructures [25]. The wavelength dependent dielectric susceptibility of gold has been taken from Johnson and Christy [22]. The Calculations were performed for the case of bottom ring outer diameter of 120 nm and top two rings of a smaller diameter 110 nm (measured extinction spectra are shown in Fig. 4). The rings have a rounded shape on top. The quartz substrate is taken into account in the calculations. To apply Green dyadic method to this complex geometry, the trimer has been meshed in volume units expanded on a hexagonal lattice with 5 nm step size. As it can be observed in the SEM images of Fig. 3, different configurations of trimers can be present, in the same processed area, and correspond to different separations of the top two rings with respect to the bottom ring. In order to take into account this experimental inhomogeneity, we have considered three situations: a bottom ring which is either separated from (5 nm distance between the ring top surfaces), touching (0 nm distance) or overlapping (10 nm overlap between the ring top surfaces) with two identical top rings separated by 15 nm. The simulation results are shown in Fig. 5.

First, one can notice that the agreement between the measured (942 nm in Fig. 4) and calculated (around 900 nm in Fig. 5) wavelengths of the near-infrared extinction band is satisfactory. In the simulations, this band appears as composed of at least two peaks with relative intensities influenced by the spatial arrangement of the rings. According to the electric near-field intensity maps (Fig. 5), computed at 850 nm, the surface plasmon field distribution strongly depends on the rings arrangement: it is confined in the gap region between the two top rings for the overlapping situation; whereas it is localized around the center of the top two rings mainly, for the touching and spacing situations. These observations are consistent with the calculations reported for nearly touching metallic nanospheres, nanoshells and nanorods [26–28]. Second, the infrared extinction band observed around 1465 nm (in Fig. 4) comes out in the calculated spectra around 1350 nm (average spectrum in Fig. 5); it is also due to strong intra-trimer electromagnetic coupling between the nanorings. From the simulated spectra (Fig. 5), this band consists of two main surface plasmon resonances with relative strengths depending on the considered interaction configuration. A change of 5 nm in the separation between the top two rings and the bottom ring causes the infrared resonances to shift by several tens of nanometers. Such a change in the interparticle spacing is of the order of the e-beam lithography resolution and strongly impacts the far field extinction spectra. Therefore, comparison between experiments and theory requires averaging of the optical spectra on the different configurations (as shown in Fig. 5).

#132979 - $15.00 USD Received 5 Aug 2010; revised 26 Sep 2010; accepted 28 Sep 2010; published 6 Oct 2010

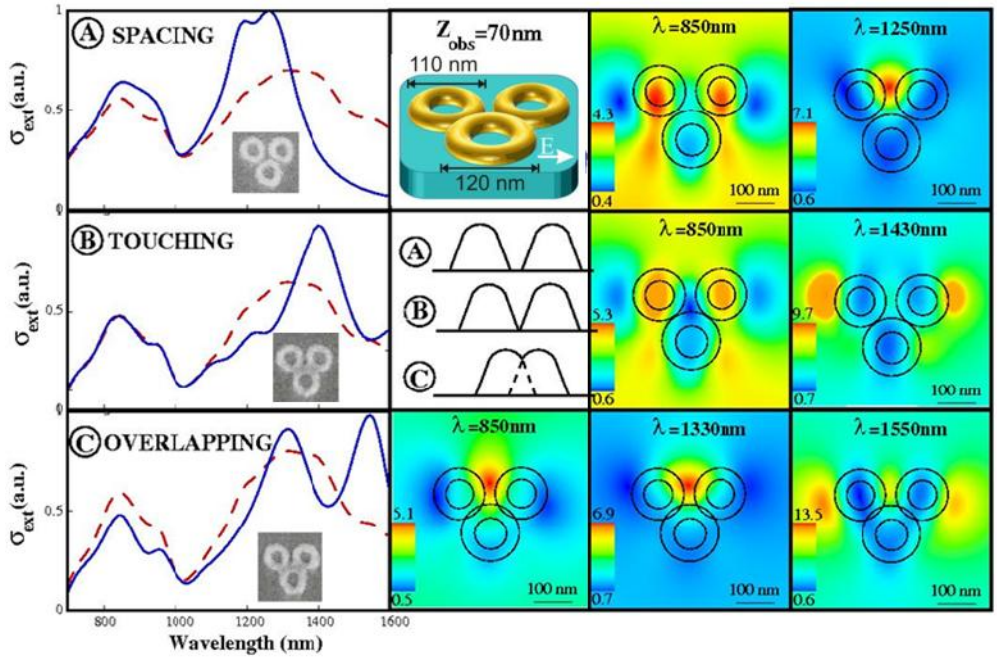

Fig. 5. Simulated extinction spectra and electric near-field intensity maps of the nanoring trimers. The computed spectra were averaged on several polarizations of the incident field in order to account for the measurements which were performed with unpolarized light. Calculations were performed for the case of bottom ring outer diameter of 120 and top two rings of a smaller diameter 110 nm. The gap between the top two rings is 15 nm. The nanorings have a rounded ring-wall shape. Three main situations are considered from our observations from SEM, where the bottom rings in trimers are separated (A), touching (B) or overlapping (C) with top two rings. The red dashed line in the left panel shows the extinction spectrum averaged over the three configurations. The electric near-field intensity maps are generated for the main SPR wavelengths and at distance Z_{obs} = 70 nm from the nanoring trimer plane. The arrow indicates the polarization of the incident electromagnetic field. The examples of corresponding SEM images of such isolated trimers are shown in the inset.

The spatial distribution of the electric field intensity around the rings (Fig. 5) changes with the spacing between the top two rings and the bottom ring. For instance, the electric near-field generated at 1250 nm for the spacing configuration is confined in the gap region between the top two rings; whereas for the touching and overlapping configurations it is mainly localized on the outer edges of the top two rings. Clearly, the arrangement of the nanorings in trimers strongly impacts the wavelength and strength of the LSPR observed in the infrared spectral range, thus providing an additional degree of freedom for tailoring the optical properties of plasmonic nanosensors. Moreover, a remarkable advantage of the trimer structure is that it provides a resonance in the infrared spectral range while preserving a high localization of the electromagnetic near-field (Fig. 5). Similar red-shifts could be obtained with elongated objects such as nanorods, but the associated electric near-field intensity is rather delocalized over the nanorod length [27]. That could be a serious limitation of nanorod based plasmonic sensors in terms of minimum number of adsorbed molecules yielding a detectable shift of the LSPR. On the contrary, in our case, the electric field is highly localized in the gap region between nano-objects. As a consequence, the detection limit should be improved using nanoring trimers which combine infrared surface plasmon resonances and strong localization of the associated electromagnetic field. In addition, the inter-trimer interaction could provide an additional strong infrared resonance suitable for surface-enhanced infrared absorption spectroscopy.

Next, we address the sensing properties of the nanoring trimers. We have studied the dependence of the LSPR on the refractive index of the medium surrounding the trimers. The

#132979 - $15.00 USD Received 5 Aug 2010; revised 26 Sep 2010; accepted 28 Sep 2010; published 6 Oct 2010

trimers were fully covered with about 100 micro-litre of solvents for chemical sensing experiments. Figure 6a shows the spectra of ring trimers (bottom ring: 120 nm diameter) in air and in pure ethanol (n = 1.398). It can be clearly observed how both LSPR shift to higher wavelengths when changing to an optically denser coating medium. Organic solvents of different refractive indices (acetone – 1.355, ethanol – 1.398, and toluene – 1.494) were chosen for the sensing experiments. The wavelength of the near-infrared LSPR is plotted in Fig. 6b as a function of the coating medium refractive index. The resonance wavelength red-shifts and scales almost linearly with the surrounding bulk refractive index unit (RIU). From a linear fit to the experimental data, we obtain an experimental sensitivity of the gold ring trimers of 345 ± 10 nm/RIU for the short-wavelength LSPR. An even much larger sensitivity can be predicted for the observed absorption peak in the mid-infrared region (1600 nm), which originates from the interactions between the rings within the trimers. Owing to the spectral limitation of the micro-spectrophotometer, we could not track the resonance of the long-wavelength surface plasmon resonance for all the coating media. However, we can compare the relative positions of the two LSPR for ethanol coating (Fig. 6a). The shadowed areas highlight the wavelength shift for the two resonances when changing the surrounding environment. As it can be seen, the shift is much larger for the longer wavelength infrared resonance ($\Delta\lambda$ = 187 nm) than for the near infrared resonance ($\Delta\lambda$ = 129 nm). This represents 45% increase in the sensitivity and could be useful for surface plasmon sensing applications.

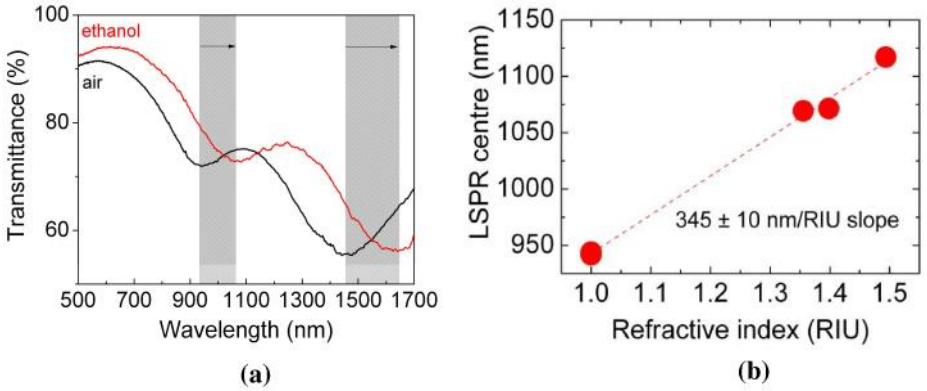

Fig. 6. (a) Transmission spectra of interacting ring trimers (bottom nanoring outer diameter of 120 nm within the trimer as shown in Fig. 4) when exposed to media of different refractive indices. The data show red-shifted LSPR with a higher refractive index medium and elucidate their potential in chemical sensing. (b) Wavelength shift of the near-infrared LSPR as a function of refractive index. The dotted line is a linear fit to the experimental data.

The sensitivity of the near-infrared SPR to the optical index of the coating medium (345 nm/RIU) here obtained for nanoring trimers is 2.65 times larger than that reported recently for nanodisk trimers with comparable size (127 nm nanodisk diameter) [20]. Indeed, the sensitivity of the LSPR associated with isolated nanodisk trimers was determined to be 130.3 nm/RIU [20]. Moreover, the surface plasmon properties of heptamers formed by interacting nanodisks have recently investigated [19]. In that study, Fano resonances, due to interferences between bright and dark plasmons, were observed and their sensitivity to the optical index of the coating medium studied. The sensitivity of the Fano dip was determined to be 300 nm/RIU which is slightly below our 345 nm/RIU obtained for the lower LSPR resonance wavelength in nanoring trimers.

4. Conclusions

In summary, we have fabricated gold nanoring trimers to tune the LSPR to the infrared spectral region while preserving a high localization of the electromagnetic energy. These nanostructured templates can be used as substrates for near-infrared SERS, surface-enhanced infrared absorption spectroscopy, and simultaneous LSPR sensing. We have shown here that

#132979 - $15.00 USD Received 5 Aug 2010; revised 26 Sep 2010; accepted 28 Sep 2010; published 6 Oct 2010

the resonance wavelengths of gold ring trimers are influenced by the ring geometry and their spacing providing a flexible tool to tune and control the spectral properties on demand. Furthermore, the sensing properties of such nanostructures to the bulk refractive index changes of environments have been also investigated. The sensitivity of the nanoring trimer SPR to the optical index of the surrounding medium was found to be much larger than that reported for nanodisk trimers [20] and comparable to that of nanodisk heptamers [19].

Acknowledgments

The authors thank funding support from Agency for Science, Technology, and Research (A*STAR) Singapore and French Embassy-Merlion Project Program. This work was supported by CALMIP computing center at Paul Sabatier University and the ETORTEK project inano from the Department of Industry of the Basque Government.

#132979 - $15.00 USD Received 5 Aug 2010; revised 26 Sep 2010; accepted 28 Sep 2010; published 6 Oct 2010